

OPTICAL SPECTRA OF FERROELECTRIC - ANTIFERROMAGNETIC
RARE EARTH MANGANATES *

K. KRITAYAKIRANA, P. BERGER and R. V. JONES
*Division of Engineering and Applied Physics,
Harvard University, Cambridge, Massachusetts 02138, USA*

Received 2 July 1969

The first optical measurement of the simultaneously ferroelectric and antiferromagnetic materials YMnO_3 , TmMnO_3 and YbMnO_3 are reported. Generally the spectra are characterized by a wide transmission window in the near infrared. For YbMnO_3 and TmMnO_3 sharp rare earth crystal field absorption lines are found within the window. As a consequence of anisotropic Mn^{3+} - Yb^{3+} exchange interaction some of the Yb^{3+} lines are exchange split. A crystal field model of the Yb^{3+} spectra is presented.

The hexagonal heavy rare earth manganates [1,2] (RMnO_3 ; R = Ho, Er, Tm, Yb, Lu and Y, Sc) exhibit a rather unique set of physical properties, and may have some potentiality for practical applications [3]. They order in triangular antiferromagnetic states [4,5] with Néel temperatures in the liquid nitrogen range. The magnetism arises mainly from the trivalent manganese [6,7], which has the $3d^4$ electronic configuration. Furthermore, these compounds are ferroelectric with high Curie temperatures [8] ($\approx 700^\circ\text{C}$) and very fast switching speeds [9] ($\approx 10^{-7}$ sec).

We report here the first optical measurements on single crystals of YMnO_3 , TmMnO_3 , and YbMnO_3 . YMnO_3 is opaque from the UV ($50\,000\text{ cm}^{-1}$) down to the near infrared. At room temperature, the absorption, which apparently is associated with Mn^{3+} , drops off at an "absorption edge" located at $10\,300\text{ cm}^{-1}$. As the temperature falls, this Urbach-like [10] absorption edge moves to higher energy, being at $12\,500\text{ cm}^{-1}$ at 4°K . Below the absorption edge, the crystal is quite transparent down to the deep infrared, where the phonon spectrum starts to rise near 1000 cm^{-1} . This wide "window" in the near infrared and the ferroelectricity of these materials should make them valuable as nonlinear optical media [11].

In TmMnO_3 and YbMnO_3 , there is superimposed on this background Mn^{3+} spectrum a host of sharp absorption lines in the window region which are due to transitions among rare earth

crystal field energy levels. In this report we concentrate our attention on the YbMnO_3 spectrum. The intensities of many of the Yb^{3+} lines show marked dependence on temperature and below the Néel temperature some of the lines split into two or more components suggestive of exchange splittings [12]. As we sketch below, we have been able to interpret the Yb^{3+} spectrum in terms of calculated crystal fields, anisotropic Mn^{3+} - Yb^{3+} exchange interactions, and phonon effects.

The compounds have the space group symmetry C_{6v}^3 ($P6_3\text{ cm}$) [1]. In the hexagonal unit cell containing six formula units, two Yb^{3+} ions occupy sites with C_{3v} local symmetry and the other four occupy the slightly more distorted sites with C_3 symmetry. The rare earth ions at both sites are 8-fold coordinated, being situated between a pair of inverted tripiramids oriented along the c -axis.

In the point charge approximation [13], we have calculated the crystal field energy levels of Yb^{3+} at both sites. The crystal field lattice sums A_n^m were performed on a digital computer including approximately 5000 ions. There is excellent convergence for all terms except A_2^0 which has a mild convergence. We used the following values of mean radii:

$$\langle r^2 \rangle = -0.022 (\text{\AA})^2 ; \quad \langle r^4 \rangle = 0.165 (\text{\AA})^4 ;$$

$$\langle r^6 \rangle = 1.064 (\text{\AA})^6$$

which are consistent, in both magnitude and sign, with the parameters for YbGG [14] and Yb:YGG [15]. These values differ significantly from

* Research supported by Advanced Research Projects Agency under Contract SD-88.

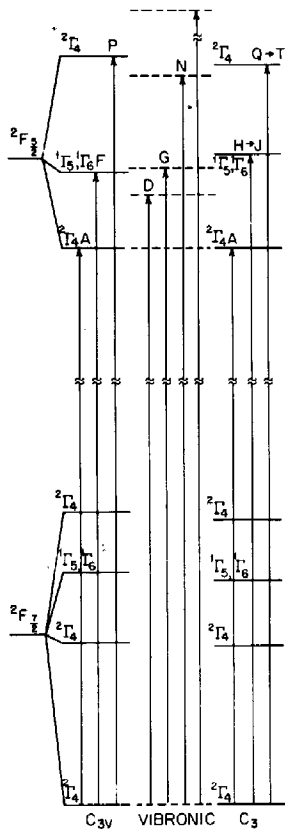


Fig. 1. Crystal field and vibronic energy levels of Yb^{3+} in YbMnO_3 .

Freeman-Watson's $\langle r^n \rangle$ [16], which did not give as good a fit to observations. We obtained the crystal field energy levels, given in fig. 1, by diagonalizing the Hamiltonian

$$H_c = \sum_{n,m} \theta_n \langle r^n \rangle A_n^m O_n^m$$

in the $|LSJ_z\rangle$ representation. Using the calculated crystal field parameters to make the assignment of line A at both sites as shown in fig. 1, all lines listed as "crystal field" in table 1 follow immediately. The poorest fit is a deviation of 1% between calculation and the center of gravity of lines Q, R, S, and T. In view of the simple nature of the point charge model, the agreement is remarkably good. As an additional measure of the reliability of the fit, the derived spin-orbit constants $\lambda = -2869 \text{ cm}^{-1}$ for C_{3v} sites and $\lambda = -2876 \text{ cm}^{-1}$ for C_3 sites compare favorably with $\lambda = -2880 \text{ cm}^{-1}$ for Yb^{3+} in YbGG [14].

From the example of the garnets [14], we expect some of the absorption lines to be phonon-related to the first strong line of electronic transition. We obtained the phonon "difference" sidebands as local maxima on the long wavelength shoulder of the first transition line A. A reflection about line A gives lines D, G, N and U as phonon "summation" sidebands of A. They involve two types of phonons, as shown in table 1.

We now turn to the most interesting feature of the Yb^{3+} spectrum, namely the exchange splitting of the crystal field spectrum. As an example of this effect, we find that the high tem-

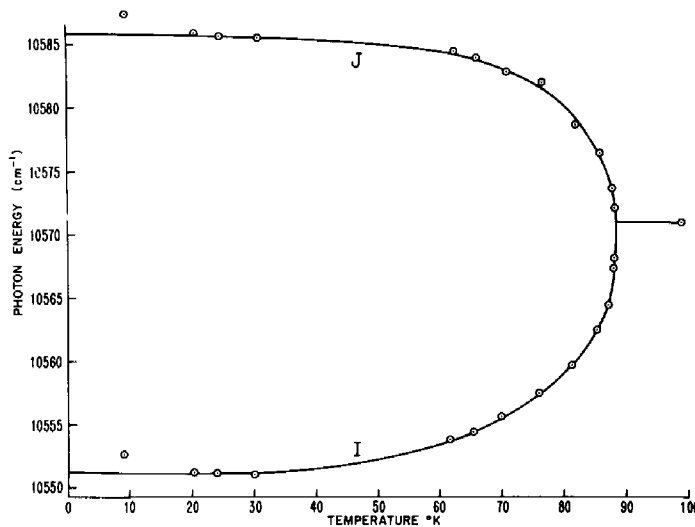


Fig. 2. Positions of lines I and J in spectrum of YbMnO_3 .

Table 1
Observed and calculated crystal field and vibronic spectrum of Yb³⁺ in YbMnO₃. Observation at 4.8°K.

Label	Observations (cm ⁻¹)	Calculations (cm ⁻¹)			Comment
		C ₃	C _{3v}	vibronic	
A	10290	10290	10290	-----	fit
D	10449	-----	-----	10444	2 phonons-I ^{a)}
F	10506	-----	10507	-----	crystal field
G	10524	-----	-----	10521	3 phonons-I ^{a)}
H	10541	}	10570	-----	crystal field exchange split
I	-----				
F'	10560				
J	10584				
N	10791	-----	-----	10796	1 phonon-II ^{b)}
P	10855	-----	10854	-----	crystal field
Q	10905	}	10829	-----	crystal field exchange split
R	10935				
S	10953				
T	10983				
U	11297	-----	-----	11302	2 phonons-II ^{b)}

a) Phonon-I = 77 cm⁻¹; b) Phonon-II = 506 cm⁻¹.

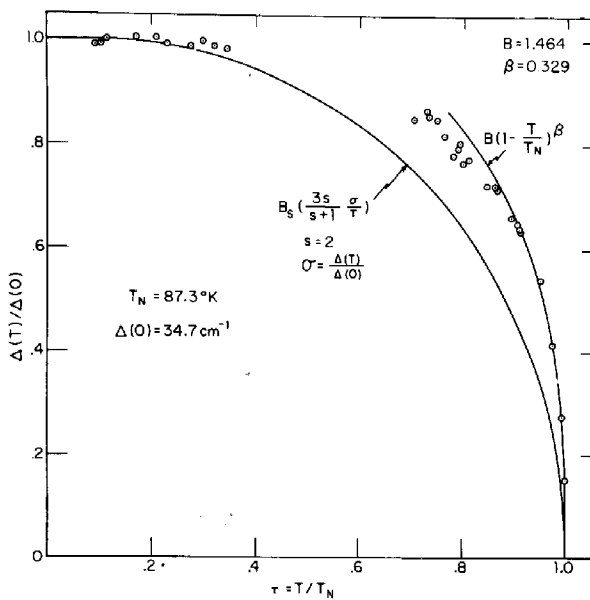


Fig. 3. Exchange splitting of Yb³⁺ crystal field transition at 10571 cm⁻¹ and critical phenomena parameters of YbMnO₃.

perature line at 10571 cm⁻¹ splits almost symmetrically into two lines below 85°K (fig. 2). Fig. 3 shows that the separation of the split lines follows a characteristic magnetization curve yielding T_N = 87.3°K for YbMnO₃ which agrees well with an intrapolation from neutron diffraction determinations of T_N of other rare earth manganates [6]. Using a zero temperature splitting of Δ(0) = 34.7 cm⁻¹, a least squares fit of the critical phenomena [17] expression

$$\Delta(T)/\Delta(0) = B(1 - T/T_N)^\beta$$

to our data in the region 0.900 < T/T_N < 0.999 gives β = 0.329, B = 1.464. Thus, we conclude that the splitting arises from an interaction between Yb³⁺ and the Mn³⁺ sublattice magnetization.

The microscopic origin of this exchange splitting may be understood by referring to fig. 4 where we note that the two rare earth sites have significantly different magnetic environments. We assume at the outset that the rare earth spin S⁰ is coupled to the Mn³⁺ spins Sⁱ_{Mn} by an anisotropic exchange interaction of the form

$$H_E = \sum_{i=1}^6 S^0 \cdot A^{(i)} \cdot S^i_{Mn}$$

where A is the exchange tensor. In a suitably

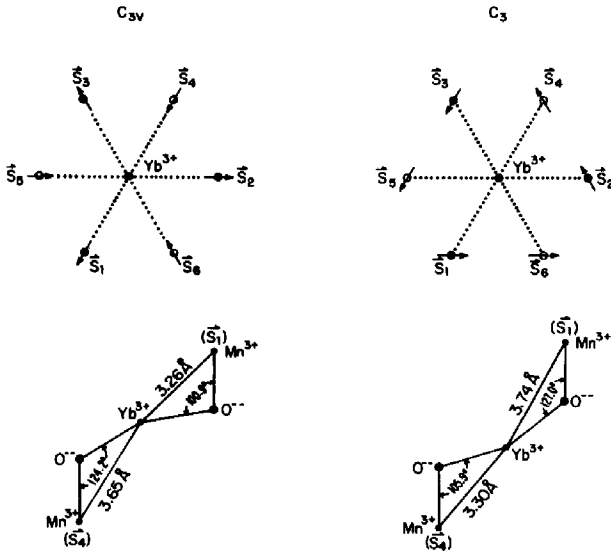


Fig. 4. Exchange fields at the two rare earth sites. S₁, S₂, S₃ above Yb³⁺, S₄, S₅, S₆ below Yb³⁺.

rotated coordinate system this Hamiltonian can be reduced to

$$H_E = 3S_z^0 (A_{zx} - A'_{zx})S \quad \text{for } C_{3v} \text{ sites,}$$

$$H_E = 3S_z^0 \left[-\frac{1}{2} (A_{zx} - A'_{zx}) + \frac{1}{2}\sqrt{3} (A_{zy} + A'_{zy}) \right] S$$

for C₃ sites, where S is the magnitude of the Mn³⁺ spin. A_{zx}, A_{zy} couple to Mn³⁺ spins above the rare earth ion and A'_{zx}, A'_{zy} to those below it. We note here that, contrary to the case of the garnets [12], the isotropic part of the exchange interactions will not give a splitting in our case at all. Furthermore, noting from fig. 3 that the

longer superexchange paths subtend more favorable angles, we expect A_{zx} and A'_{zx} to be nearly equal and arrive at the remarkable conclusion that there should be a negligible splitting at C_{3v} sites and a finite splitting at C₃ sites. This expectation is confirmed by our observation.

REFERENCES

- [1] H. L. Yakel, W. C. Koehler, E. F. Bertaut and E. F. Forrat, Acta Cryst. 16 (1963) 957.
- [2] E. F. Bertaut, E. F. Forrat and P. Fang, Compt. Rend. Acad. Sci. (Paris) 256 (1963) 1958.
- [3] P. Guinet, Ph. Coeure and E. F. Bertaut, in: Colloq. internat. tech. memoires (Vesoul, 1965) p. 320.
- [4] E. F. Bertaut, M. Mercier and R. Pauthenet, J. Phys. 25 (1964) 550.
- [5] S. A. Kizhaev, V. A. Bokov and O. V. Kackalov, Soviet Phys.-Solid State 8 (1966) 215.
- [6] W. C. Koeler, H. L. Yakel, E. O. Wollan and J. W. Cable, Phys. Letters 9 (1964) 93.
- [7] T. Penney, P. Berger and K. Kritayakirana, J. Appl. Phys. 40 (1969) 1234.
- [8] I. G. Ismailzade and S. A. Kizhaev, Soviet Phys. Solid State 7 (1965) 236.
- [9] Ph. Coeure, J. Phys. 28 (1967) 339.
- [10] J. J. Hopfield, Comments Solid State Phys. 1 (1968) 16.
- [11] P. H. Fang, NASA Goddard Space Flight Center, Tech. Rept. N65-29473 (1964), unpublished.
- [12] K. A. Wickersheim and R. L. White, Phys. Rev. Letters 8 (1962) 483.
- [13] M. T. Hutchings, in: Solid state physics, vol. 16, eds. F. Seitz and D. Turnbull (Academic Press, New York, 1964).
- [14] R. A. Buchanan, K. A. Wickersheim, J. J. Pearson and G. F. Herrman, Phys. Rev. 159 (1967) 245, 251.
- [15] M. T. Hutchings and W. P. Wolf, J. Chem. Phys. 41 (1964) 617.
- [16] A. J. Freeman and R. E. Watson, Phys. Rev. 127 (1962) 2058.
- [17] P. Heller, Rept. Progr. Phys. 30 (1967) 731.